Pulse-Profile-Maintaining Characteristics of Gain-Switched Nanosecond Raman Fiber Laser and Amplifier

Haoqian Wu, Junqing Zhao, Deqin Ouyang, Yewang Chen, Minqiu Liu, Qitao Lue, and Shuangchen Ruan

***Abstract*—This paper investigates pulse-profile-maintaining characteristics of a gain-switched nanosecond Raman fiber laser (RFL) and its Raman fiber amplifier (RFA). It is found that the pulse profiles can be precisely maintained after the gain-switched Raman conversion, only if the pump pulse repetition frequency (PRF) is an integer multiple of, a unit fraction of, or multiple unit fractions of the fundamental cavity-defined PRF. The produced Raman pulses are then amplified in an RFA, and the pulse profiles can also be precisely maintained. However, it is further noticed that the detuning-induced defects can be amplified if they are with the pulse itself. All these observed phenomena should originate from the transient property of Raman gain, not involving any notable delaying or saturation effects that are typically seen with rare-earth-doped gain fibers. Our results demonstrate that, in the nanosecond scale, the Raman-converted pulse can well maintain its profile and shows strong resistance to detune between PRFs of the pump and Raman pulses. Benefiting from that, we can reasonably neglect the pump depletion effect due to walk-off effect typically seen in various short pulse regimes, which can largely simplify the design of nanosecond pulsed pumping Raman sources.**

***Index Terms*—Fiber lasers, laser amplifiers, stimulated Raman scattering.**

I. Introduction

FIBER laser is attracting more and more attention in scientific research, biomedical and industrial applications, etc., due to its unique advantages such as compactness, high efficiency, and high flexibility [1]–[3]. But, there are some wavelength ranges that cannot be achieved limited by the emission range of rare earth ions. Stimulated-Raman-scattering (SRS)-based Raman fiber laser (RFL) has a gain frequency range of as wide as ∼40 THz [4], and the emission wavelength of Raman Stokes light is determined by the pump wavelength and Raman frequency shift of the used fiber. RFL has been considered as a superior option for achieving arbitrary lasing wavelength within the fiber-transparent window. Great breakthroughs have been made in high power continuous wave (CW) RFL and Raman fiber amplifier (RFA) [5]–[10].

Nanosecond pulses from an RFL have special applications in lidar measurement, multi-photon microscopy, optical coherence tomography, *etc*. Nanosecond pulses can typically be achieved through gain-switching, Q-switching or mode-locking. In terms of the complexity of the RFL cavity, the Q-switched or mode-locked technique requires modulation components such as acousto-optic modulator [11]–[14], electro-optic modulator [15], or saturable absorbers [16]–[18] et al.

Compared to the Q-switched method, gain-switched pulsed RFLs have many advantages, such as easily tunable pulse duration and pulse repetition frequency (PRF), simple structure without any modulation components, and flexible operation wavelength. For the gain-switched fiber laser, there have been lots of investigations based on ytterbium, erbium, thulium, and holmium-doped gain fibers [19]–[23], including fluoride fiber in the mid-infrared region [24]–[26]. However, the reports on gain-switched RFL are still rarely seen. In 2007, A. S. Kurkov et al. realized a gain-switched RFL though cascaded conversion from a passively Q-switched Yb-doped fiber laser. And, the output Raman pulse duration was microsecond level due to the large pump pulse duration of 3 μs [16]. For the nanosecond Raman pulse generation, in the year of 2015, Yao et al. constructed a pulsed Raman fiber amplifier at 1686 nm pumped by an actively Q-switched Er/Yb co-doped fiber laser. The Raman gain fiber used was a segment of graded-index multimode fiber with core and cladding diameter of 50 μm and 125 μm, respectively. The obtained Raman pulse duration was 139 ns with the maximum first order Stokes average power of 4.4 W. This is the maximum output power of the gain-switched RFL have reported [9]. In 2021, C. Quan et al. reported a gain-switched RFL with several nanosecond pulse generation by using a 1550 nm PRF tunable pulsed laser as the pump source and 1 km single-mode fiber (SMF) as the Raman gain medium. The RFL pulse duration increased from 4.41 ns to 7.47 ns with the increase of pump power [27]. However, these reports did not investigate the pulse-profile relation between the pump and Raman-converted pulses.

Manuscript received 8 July 2022; revised 28 July 2022; accepted 28 July 2022. Date of publication 2 August 2022; date of current version 15 August 2022. This work was supported in part by the National Natural Science Foundation of China under Grant 61905146 and in part by the Shenzhen Key Project for Technology Development under Grants JSGG20190819175801678 and JSGG20191129105838333. *(Corresponding author: Deqin Ouyang.)*

Haoqian Wu, Junqing Zhao, Deqin Ouyang, Yewang Chen, Minqiu Liu, and Shuangchen Ruan are with the Key Laboratory of Advanced Optical Precision Manufacturing Technology of Guangdong Higher Education Institutes, Shenzhen Technology University, Shenzhen 518118, China (e-mail: haoqian_wu@foxmail.com; junqingzhao@outlook.com; ouyangdeqin@sztu.edu.cn; chenyewang@sztu.edu.cn; 544219936@qq.com; scruan@sztu.edu.cn).

Qitao Lue is with the HAN's Laser, Shenzhen 518057, China, and also with the Key Laboratory of Advanced Optical Precision Manufacturing Technology of Guangdong Higher Education Institutes, Shenzhen Technology University, Shenzhen 518118, China (e-mail: lvqitao@sztu.edu.cn).

Digital Object Identifier 10.1109/JPHOT.2022.3195757

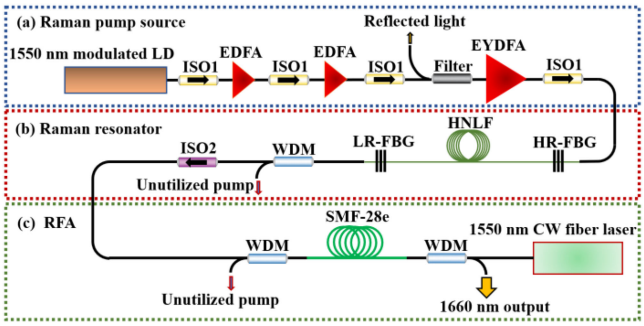

Fig. 1. Schematic configuration of (a) Raman pump source. (b) Raman resonator. (c) RFA. LD: laser diode, ISO1: 1550 nm optical isolator, EDFA: Erbium-doped fiber amplifier, Filter: 1550 nm optical bandpass filter, EYFDA: Erbium/Ytterbium co-doped fiber amplifier, HR-FBG: high-reflectivity FBG, LR-FBG: low-reflectivity FBG, WDM: 1550/1660 nm wavelength-division multiplexing coupler, ISO2: 1660 nm optical isolator.

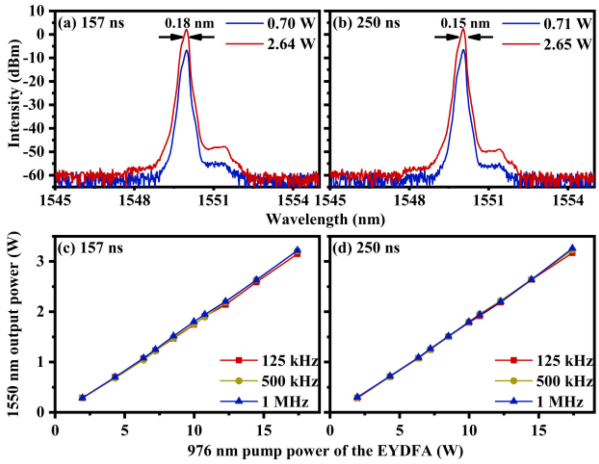

Fig. 2. Raman pump source spectra at different output powers when the PRF is set to 500 kHz, and the seeding pulse duration is set to (a) 157 ns, and (b) 250 ns, respectively. (c) and (d): Related output average power characteristics of the EYDFA versus the incident pump power.

It has been well known that in pulsed pumping Raman fiber sources various effects like walk-off, group velocity dispersion (GVD), etc. [28] can severely decrease the Raman-conversion efficiency through pump depletion it the related pulse duration is short down to nanosecond or even less. However, to date no detailed investigation can be found how much effect can be induced with if the pulsed pumping is within the nanosecond regime, although there exist some theoretically vague arguments or some related yet unclear experimental descriptions. For that, in this paper, we investigate in detail on the pulse dynamics of a gain-switched RFL regarding to the pump pulse as well as its further Raman amplification.

II. Experimental Setup

The schematic configuration of the 1.66 μm gain-switched RFL is shown in Fig. 1, which consists of three parts: (a) Raman pump source, (b) Raman resonator, and (c) RFA. The Raman pump source which is a master oscillator power-amplifier (MOPA) system at 1.55 μm and consists of an electrically modulated laser diode (LD) as the seeding source, two single-mode erbium-doped fiber amplifiers (EDFAs), and an erbium-ytterbium-doped double-clad fiber amplifier (EYDFA). The pump source of 1st and 2nd EDFA are both a 200 mW, 976 nm single-mode LD, and the pump source of EYDFA is a 20 W, 976 nm multi-mode LD. In case of the adverse effects of backward light, several isolators are used before and after each fiber amplifier. A bandpass filter with central wavelength of 1550 nm and bandwidth of 4 nm is used to block the amplified spontaneous emission (ASE) after the second EDFA. The PRF and pulse duration of the modulated LD can be adjusted within 1-1000 kHz and 5-250 ns, respectively.

Fig. 1(b) shows the Raman resonator, which is consisted of a pair of fiber Bragg gratings (FBGs) and a piece of high nonlinearity fiber (HNLF, UHNA7) as Raman gain medium. The core/cladding diameter and core NA of the UHNA 7 fiber are 2.4/125 μm and 0.41, respectively. The calculated nonlinear coefficient is $\sim$5.27 $(\mathrm{W{\cdot}km})^{-1}$ at 1660 nm. The Raman gain coefficient should be roughly the typical value of 1×10^{-13} m/W [28]. The central wavelength, bandwidth, and reflectivity of the high reflection FBG (HR-FBG) are 1660.12 nm, 0.53 nm, and 99.77%, respectively. Correspondingly they are 1660.12 nm, 0.25 nm, and 54.0%, respectively, for the low reflection FBG (LR-FBG). The center wavelength of the FBGs match the Raman shift peak (430 cm^{-1}) of the UHNA7 fiber with a pump wavelength of 1550 nm. The used length of the HNLF is $\sim$203 m (including the pigtails of FBG), corresponding to the PRF of 500 kHz. The 500kHz-PRF not only enables a wide range of PRF regulation, but also avoids the complex nonlinear effects caused by a low PRF. A 1550/1660 nm WDM is used to spectrally separate the first-order Stokes light and the residual pumping light.

The RFA with a backward pump scheme is depicted in Fig. 1(c). We used a CW fiber laser system at 1550 nm as the pump source. A piece of $\sim$9 km long SMF (SMF-28e, Corning, Inc.) provides the Raman gain. A high power 1550/1660 nm WDM is used to couple the pump light and separate the amplified first order Raman stokes light. And another WDM on the right side was utilized to separate the residual pump light.

In the experiment, the pulse train and single pulse profiles are measured via a 12.5 GHz InGaAs photodetector (EOT, ET-5000F) combined with a 4 GHz bandwidth oscilloscope (Teledyne Lecroy, WaveRunner 8404M). The optical spectrum of the oscillator is measured by an optical spectrum analyzer (YOKOGAWA, AQ6375B).

III. Result and Discussion

A. Raman Pump Source

A PRF and pulse duration tunable 1550 nm fiber amplifier seeded by a modulated LD was utilized as the pump source for the gain-switched RFL. Fig. 2(a) and (b) show the spectra of the Raman pump source at different output power when the PRF is set to 500 kHz with duration of 157 ns and 250 ns, respectively. It can be seen that the amplified spectra have no significant broadening. This indicates that there is no significant amplified spontaneous emission (ASE) or nonlinear effect during the pulse amplification. Fig. 2(c) and (d) show the evolutions of the

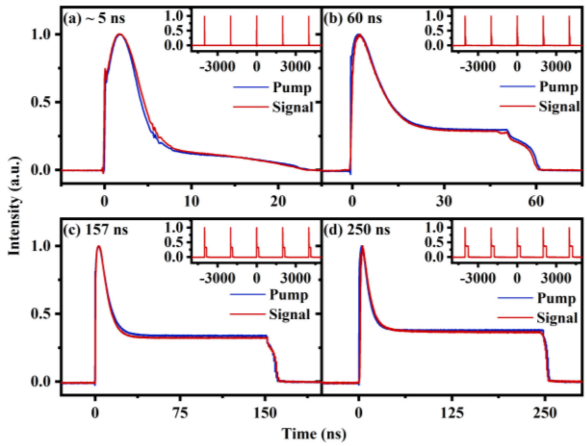

Fig. 3. Comparison of pulse profiles before and after Raman frequency conversion when PRF is set to 500 kHz with pulse durations of (a) ~5 ns, (b) 60 ns, (c) 157 ns, and (b) 250 ns, respectively.

average output power of the Raman pump source with the pump power at different PRFs and durations, all sharing roughly the same slope efficiency of ~17.5%.

B. PRF and Duration Related Temporal Characteristics of Gain-Switched Raman Pulses

Fig. 3 comparatively plots the gain-switched Raman pulses against their corresponding pump pulses with several different durations. As seen, both the two sets of pulses show a type of h-shaped pulse profile, originating from the temporally dependent gain during pulse amplification of the fiber pump source. The seeding PRF of the pump source is set at 500 kHz, which just corresponds to the fundamental PRF of the constructed RFL that has a cavity length of ~203 m. It can be clearly seen that each Raman-converted pulse can precisely maintain the profile of the launched gain-switching pump pulse, especially when the pulse becomes longer. This indicates that the Raman conversion process is transient and shows no delaying effect. Such a transient gain is quite different from typical rare-earth-doped fibers which always involve saturation effect and even complex temporal dependences as for pulse amplification [29], [30].

We further investigated how the PRF of the pump source can affect the gain-switched Raman pulse profiles through setting the pump PRF at several values: 125 kHz, 250 kHz, 333 kHz, 455 kHz, 500 kHz, 566 kHz, 714 kHz, and 1 MHz; the results are shown in Fig. 4. It can be clearly seen that the pulse profile can be well maintained only when the setting PRF is a quarter, a half, two thirds, or an integer multiple of the fundamental PRF of the RFL cavity, as shown in Fig. 4(a), (b), (c), (e), and (h). Otherwise, some defects appear on the pulse profile or between two successive pulses as seen in Fig. 4(d), (f), and (g), where each pump PRF is an ill-defined fraction of the fundamental PRF.

Fig. 5 plots the output spectra at different PRFs corresponding to Fig. 4. For each PRF, only the 1st-order Stokes line can be excited when the pump power and also the output power is low. As the pump power increases, the 2nd-order Stokes line

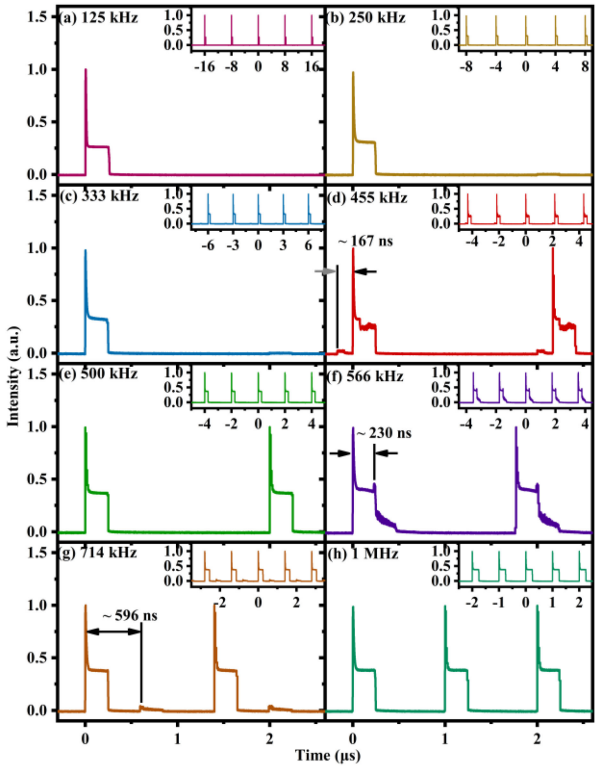

Fig. 4. Raman gain-switched pulse temporal characteristic when the pulse duration is set to 250 ns, and PRF is set to (a) 125 kHz, (b) 250 kHz, (c) 333 kHz, (d) 455 kHz, (e) 500 kHz, (f) 566 kHz, (g) 714 kHz, and (h) 1 MHz, respectively (Insert: corresponding pulse train).

appears; meanwhile, the Raman spectra of both the 1st and 2nd-order Stokes lines become increasingly wider due to the accompanying self-phase modulation (SPM).

We have also investigated the related temporal characteristics at different pump pulse duration. When the pump pulse duration is reduced to 157 ns, the temporal characteristics of the Raman gain-switched pulses are similar to those with the previously 250 ns pump pulses. But now the defects on the pulses largely disappear when the PRF detune occurs. Alternatively, those defects only shifted to somewhere between two successive pulses in form of a much-lowered sub-pulse, as seen in Fig. 4(d), (f), and (g). This should be mainly due to that the temporally pulse mismatching due to the PRF detune is beyond the local pulse duration.

Another notable point in Fig. 6 is that the ratio between the peak to the pedestal parts varies remarkably with the change of PRF. This is due to the similar change with the incident pump pulse. Although the pump pulse remains the same pedestal width as the change of PRF, the ratio between the peak to the pedestal parts changes significantly with repetition rate. This characteristic is due to the pump source itself. Each gain-switched pulse profile still well follows the profile of the used pump pulse, similar to the comparative characteristics depicted in Fig. 3.

The output power characteristics of 1st-order Stokes Raman light are given in Fig. 7. The maximum output power obtained is 177.6 mW with the pulse width and PRF of 250 ns and 500 kHz, respectively. At higher pump powers, the drop in conversion

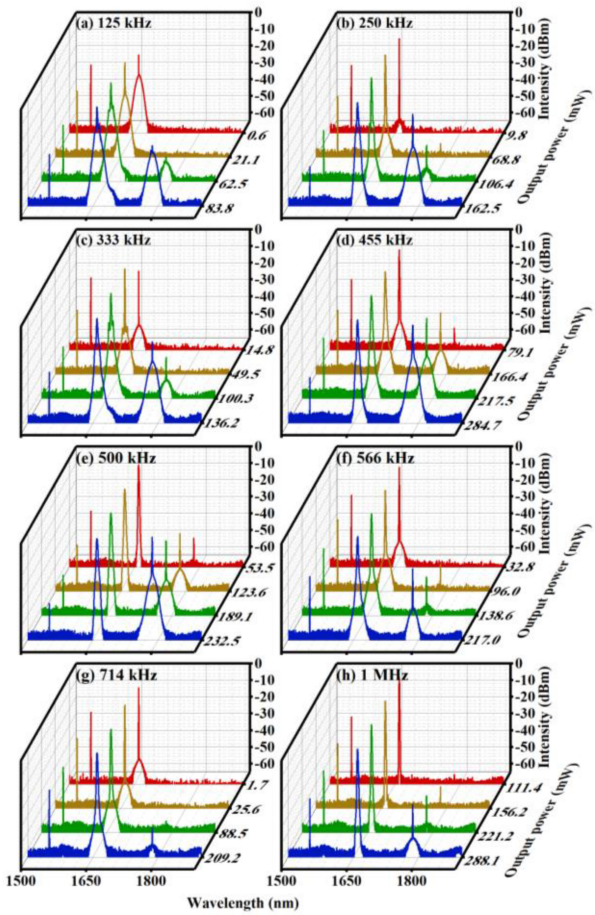

Fig. 5. Raman gain-switched pulse spectrum when the pump pulse duration is set to 250 ns, and PRF is set to (a) 125 kHz, (b) 250 kHz, (c) 333 kHz, (d) 455 kHz, (e) 500 kHz, (f) 566 kHz, (g) 714 kHz, and (h) 1 MHz, respectively.

efficiency caused by the emergency of 2nd-order Stokes Raman light. And, the same power characteristics can be found for the pulse width of 157 ns.

C. RFA

Fig. 8 depicts amplification characteristics of the Raman pulses at several pump PRFs. As seen in Fig. 8(a) and (d), no notable profile change can be observed if the PRF is a quarter or an integer multiple of the fundamental PRF of the original RFL. The defects on the local Raman pulse, however, see obvious amplification as seen in Fig. 8(b) where the spike on the pulse trailing edge becomes considerably higher. But, interestingly, the defects between two successive pulses experience no amplification as shown in Fig. 8(c). These characteristics are mainly due to that the Raman gain is peak-power-related. The defect will experience a high instantaneous Raman gain due to the high peak power if it appears on the pulse. However, it can only acquire a negligible Raman gain if it appears between two successive pulses due to the much lowered peak power. As seen in Fig. 8(b) and (c), the contrast ratio between the peak powers of the defects appearing on the pulse and besides the pulse can reach ~21.4.

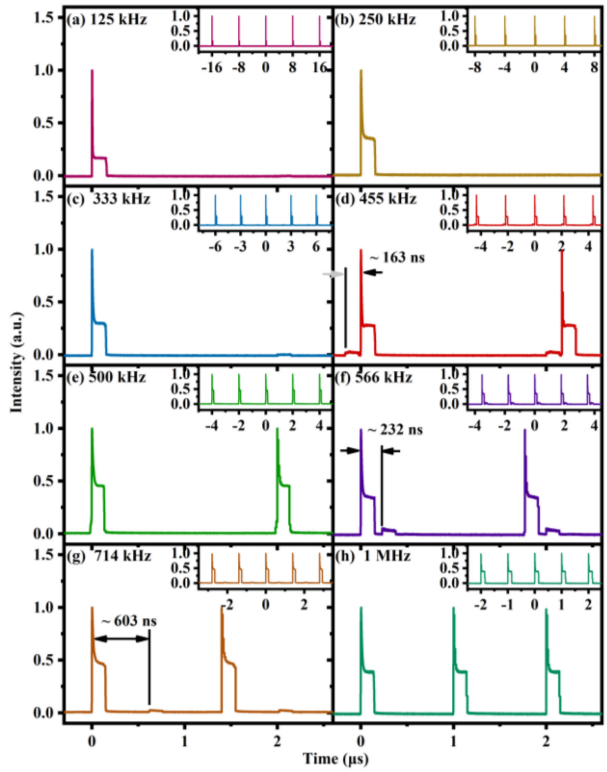

Fig. 6. Gain-switched Raman pulses at the pump pulse duration of 157 ns, and PRF of (a) 125 kHz, (b) 250 kHz, (c) 333 kHz, (d) 455 kHz, (e) 500 kHz, (f) 566 kHz, (g) 714 kHz, and (h) 1 MHz, respectively.

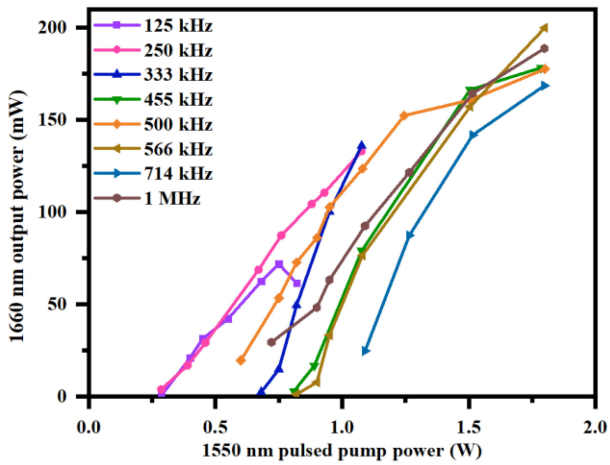

Fig. 7. Output power of the Raman resonator with the pulse duration of 250 ns at different PRFs.

Fig. 8(e) through (h) plot the corresponding spectra before and after Raman amplification. Significant spectral broadening can be observed. At 250 kHz PRF, the amplified spectrum even broadens to a supercontinuum-like span covering over 100 nm wavelength region. The main effect that causes the spectral broadening around the 1st-order Stokes Raman light, as seen in Fig. 8(e) through (h), should be the SPM. The SPM effect is stronger if the pulse repetition rate is lower due to the associated higher peak power. At the 250 kHz repetition rate, the peak power is further high enough to excite the 2nd-order Stokes

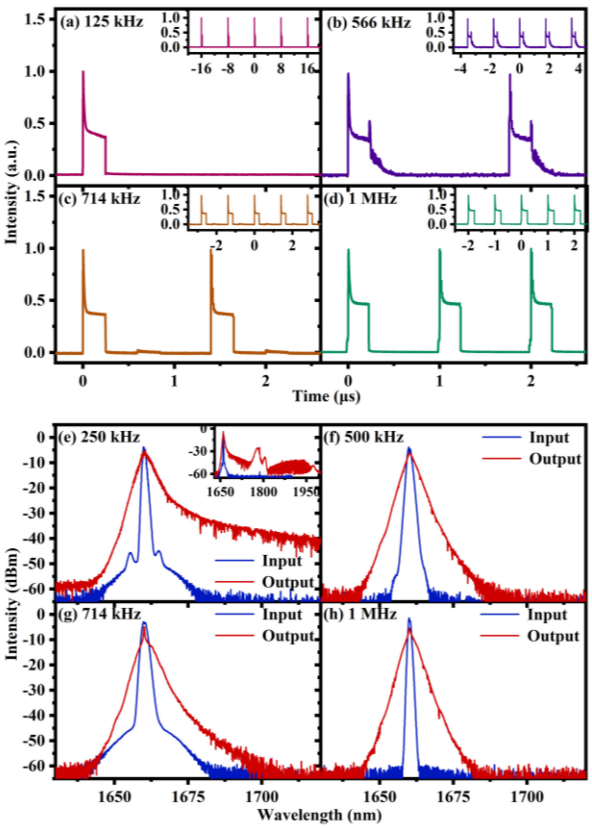

Fig. 8. Amplified gain-switched Raman pulses with the same duration of 250 ns and PRFs of (a) 125 kHz, (b) 566 kHz, (c) 714 kHz, and (d) 1 MHz, respectively. (e)-(h): The corresponding spectra before and after Raman amplification.

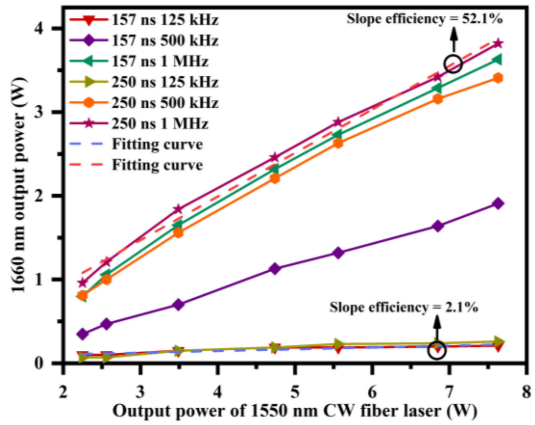

Fig. 9. Output power of the RFA at different PRFs and pulse durations.

Raman light, which together with the related SPM caused the supercontinuum-like spectrum generation, as seen in Fig. 8(e).

We also measured the power conversion efficiency in the RFA. Although all the pulse profiles are not rectangular, the pulse duty circle (PDC) still relates to the conversion efficiency directly. Fig. 9 demonstrates the power evolution of the RFA against the incident CW pump power. As seen, comparatively the 250 ns-1 MHz pulse train that have the largest PDC reaches the highest slope efficiency of ∼52.1%, while the 157 ns-125 kHz one with the minimum duty cycle achieves the lowest efficiency of ∼2.1%. The obtained highest Raman power is ∼3.8 W with pulse duration and PRF of 250 ns and 1 MHz, respectively.

In fact, for our used extremely long (∼9 km) piece of Raman fiber, the associated Raman threshold is roughly 1.3 W [28]. Even some more details might be slightly different from that in Ref. [28], it should be reasonably less than 2 W. Thus, our used 8 W pump is adequate to realize Raman effect and meanwhile the achieved high conversion efficiency is also predictable. Another noted point is that our mentioned slope efficiency here is the overall case which include both the power directly from the Raman oscillator and also the newly produced Raman power. Considering that the Raman threshold has been reached, there should be some newly produced CW Raman light besides the pulsed Raman light produced during the PDC. The continuous wave Raman light is produced during the backward pumping and then reflected back as the output through the distributed feedback Rayleigh scattering effect [31], [32]. But temporally we do not have proper equipment to measure how much power is contained as the CW. All these three factors contribute to the high slope efficiencies as achieved in Fig. 9.

IV. Conclusion

In conclusion, we have demonstrated the temporal characteristics of gain-switched RFL and its further RFA. Pulse-profile-maintaining characteristics were observed when the pump PRF is in-tune with, a multiple of, or some particular fraction of the cavity-defined fundamental PRF of the RFL. We also investigated the PRF detuning characteristics where pulse-duration-dependent defects either on the Raman-converted pulses or in the pulse intervals can be observed. The temporal evolutions of the further RFL are then further characterized. Our results show that in the nanosecond regime, we do not have to concern too much about the pump depletion due to various temporal walk-off effects that are typically much considerable with short pulse regimes. However, still we have to pay enough attention to the frequency detuning effects in both the RFL and RFA, which can cause some deleterious effects on the generated pulse profile. Our results can provide some useful insights to the design of pulsed pumping Raman fiber sources.

References

[1] G. Mourou, B. Brocklesby, T. Tajima, and J. Limpert, "The future is fibre accelerators," *Nature Photon.*, vol. 7, pp. 258–261, 2013.
[2] J. Gabzdyl, "Fibre lasers make their mark," *Nature Photon.*, vol. 2, pp. 21–23, 2008.
[3] C. Jauregui, J. Limpert, and A. Tünnermann, "High-power fibre lasers," *Nature Photon.*, vol. 7, pp. 861–867, 2013.
[4] D. Hollenbeck and C. D. Cantrell, "Multiple-vibrational-mode model for fiber-optic Raman gain spectrum and response function," *J. Opt. Soc. Amer. B*, vol. 19, no. 12, pp. 2886–2892, 2002.
[5] D. J. Richardson, J. Nilsson, and W. A. Clarkson, "High power fiber lasers: Current status and future perspectives," *J. Opt. Soc. Amer. B*, vol. 27, pp. B63–B92, 2010.
[6] L. Zhang, J. Dong, and Y. Feng, "High-power and high-order random Raman fiber lasers," *IEEE J. Sel. Topics Quantum Electron.*, vol. 24, no. 3, May/Jun. 2018, Art. no. 1400106.
[7] Y. Chen, T. Yao, H. Xiao, J. Leng, and P. Zhou, "High-power cladding pumped Raman fiber amplifier with a record beam quality," *Opt. Lett.*, vol. 45, no. 8, pp. 2367–2370, 2020.
[8] H. Jiang, L. Zhang, and Y. Feng, "Silica-based fiber Raman laser at >2.4 μm," *Opt. Lett.*, vol. 40, no. 14, pp. 3249–3252, 2015.

[9] W. Yao, B. Chen, J. Zhang, Y. Zhao, H. Chen, and D. Shen, "High-average-power operation of a pulsed Raman fiber amplifier at 1686 nm," *Opt. Exp.*, vol. 23, no. 9, pp. 11007–11012, 2015.
[10] J. Liu et al., "Short-pulsed Raman fiber laser and its dynamics," *Sci. China Phys. Mech. Astron.*, vol. 64, 2021, Art. no. 214201.
[11] J. Ye, J. Xu, H. Zhang, J. Wu, and P. Zhou, "Wavelength-tunable Q-switched Raman fiber laser," *Laser Phys.*, vol. 28, 2018, Art. no. 035108.
[12] A. G. Kuznetsov, E. V. Podivilov, and S. A. Babin, "Actively Q-switched Raman fiber laser," *Laser Phys. Lett.*, vol. 12, 2015, Art. no. 035102.
[13] J. Xu et al., "Narrow-linewidth Q-switched random distributed feedback fiber laser," *Opt. Exp.*, vol. 24, no. 17, pp. 19203–19210, 2016.
[14] X. Yang, L. Zhang, H. Jiang, T. Fan, and Y. Feng, "Actively mode-locked Raman fiber laser," *Opt. Exp.*, vol. 23, no. 15, pp. 19831–19836, 2015.
[15] M. Bravo, M. Fernandez-Vallejo, and M. Lopez-Amo, "Internal modulation of a random fiber laser," *Opt. Lett.*, vol. 38, no. 9, pp. 1542–1544, 2013.
[16] A. S. Kurkov, V. V. Dvoyrin, V. M. Paramonov, O. I. Medvedkov, and E. M. Dianov, "All-fiber pulsed Raman source based on Yb:Bi fiber laser," *Laser Phys. Lett.*, vol. 4, no. 6, pp. 449–451, 2007.
[17] N. Hisamuddin, U. N. Zakaria, M. Z. Zulkifli, A. A. Latiff, H. Ahmad, and S. W. Harun, "Q-switched Raman fiber laser with molybdenum disulfide-based passive saturable absorber," *Chin. Phys. Lett.*, vol. 33, no. 7, 2016, Art. no. 074208.
[18] W. Pan, J. Zhou, L. Zhang, and Y. Feng, "Rectangular pulse generation from a mode locked Raman fiber laser," *J. Lightw. Technol.*, vol. 37, no. 4, pp. 1333–1337, Feb. 2019.
[19] R. Petkovšek, V. Agrež, D. Sangla, J. Saby, R. B. Picard, and F. Salin, "Gain-switched ytterbium-doped rod-type fiber laser," *Laser Phys. Lett.*, vol. 11, no. 10, 2014, Art. no. 105808.
[20] Y. Hou, Q. Zhang, S. Qi, X. Feng, and P. Wang, "Monolithic all-fiber repetition-rate tunable gain-switched single-frequency Yb-doped fiber laser," *Opt. Exp.*, vol. 24, no. 25, pp. 28761–28767, 2016.
[21] C. Guo et al., "Tunable passively-synchronized 1-μm Q-switched and 1.5-μm gain-switched dual-wavelength fiber laser based on an Er/Yb codoped fiber," *IEEE Photon. J.*, vol. 9, no. 3, Jun. 2017, Art. no. 1502609.
[22] M. Jiang and P. Tayebati, "Stable 10 ns, kilowatt peak-power pulse generation from a gain-switched Tm-doped fiber laser," *Opt. Lett.*, vol. 32, no. 13, pp. 1797–1799, 2007.
[23] H. Luo, F. Liu, J. Li, and Y. Liu, "High repetition rate gain-switched Ho-doped fiber laser at 2.103 μm pumped by h-shaped mode-locked Tm-doped fiber laser at 1.985 μm," *Opt. Exp.*, vol. 26, no. 20, pp. 26485–26494, 2018.
[24] C. Wei, H. Luo, H. Shi, Y. Lyu, H. Zhang, and Y. Liu, "Widely wavelength tunable gain-switched Er^{3+}-doped ZBLAN fiber laser around 2.8 μm," *Opt. Exp.*, vol. 25, no. 8, pp. 8816–8827, 2017.
[25] F. Jobin, V. Fortin, F. Maes, M. Bernier, and R. Vallée, "Gain-switched fiber laser at 3.55 μm," *Opt. Lett.*, vol. 43, no. 8, pp. 1770–1773, 2018.
[26] H. Luo et al., "Watt-level gain-switched fiber laser at 3.46 μm," *Opt. Exp.*, vol. 27, no. 2, pp. 1367–1375, 2019.
[27] C. Quan, Z. Hu, D. Wu, R. Wang, S. Dai, and Q. Nie, "Short-pulse gain-switched Raman fiber laser based on conventional silica fiber," *Opt. Laser Technol.*, vol. 141, 2021, Art. no. 107154.
[28] G. Agrawal, *Nonlinear Fiber Optics*, 6th ed., San Diego, CA, USA: Academic, 2019.
[29] J. Zhao et al., "100 W dissipative soliton resonances from a thulium-doped double-clad all-fiber-format MOPA system," *Opt. Exp.*, vol. 24, no. 11, pp. 12072–12081, 2016.
[30] P. Sidorenko and F. Wise, "Generation of 1 μJ and 40 fs pulses from a large mode area gain-managed nonlinear amplifier," *Opt. Lett.*, vol. 45, no. 14, pp. 4084–4087, 2020.
[31] D. V. Churkin et al., "Raman fiber lasers with a random distributed feedback based on Rayleigh scattering," *Phys. Rev. A*, vol. 82, no. 3, 2010, Art. no. 033828.
[32] Y. Zhang et al., "Low quantum defect random Raman fiber laser," *Opt. Lett.*, vol. 47, no. 5, pp. 1109–1112, 2022.